

## Interplay of Stress, Structure, and Stoichiometry in Ge-Covered Si(001)

Feng Liu and M. G. Lagally

*University of Wisconsin, Madison, Wisconsin 53706*

(Received 15 November 1995)

By calculating the evolution of surface energies and surface stress tensors of Ge-covered Si(001) with increasing Ge coverage, we derive the most probable Ge stoichiometry in the subsurface regions beyond 1 monolayer coverage. We compare the calculated surface reconstruction and surface stress at the thermodynamic and kinetic limits to experiment to provide a quantitative understanding of the recently observed Ge-induced reversal of surface stress anisotropy. [S0031-9007(96)00004-X]

PACS numbers: 68.35.Md, 68.35.Bs, 68.35.Gy

Si(001) exhibits a wealth of fascinating and intriguing phenomena in which surface stress often plays an important role. For clean Si(001), the presence of an anisotropic surface stress tensor gives rise to a ground-state stress-domain structure, consisting of equally populated  $1 \times 2$  and  $2 \times 1$  domains [1,2]. For Ge-covered Si(001), the distribution of the stress (strain) field in the overlayer regions, greatly enhanced by lattice mismatch, has been shown to be responsible for the  $2 \times N$  reconstruction [3–5], interlayer mixing [6–8], step roughening [9] and step bunching [10], and the transition from layer growth to three-dimensional cluster growth [3,7,11,12]. The driving forces generated by surface stress and its anisotropy introduce various changes in surface morphology, which in turn modify the stress field. The control of surface stress through control of the amount of deposited Ge can lead to novel surface properties. For example, a recent experiment [13] shows that the intrinsic surface stress anisotropy of Si(001) can be tuned through zero and reversed in sign by Ge deposition.

Despite extensive studies [1–13] on surface morphology and surface stress of Ge-covered Si(001), there are significant gaps in our understanding of the morphology and stress relationship in the Ge/Si(001) system. Fundamental in those gaps is the stoichiometry of the surface and subsurface regions as the coverage of Ge changes. It is difficult to distinguish between Si and Ge because of their similar atomic, electronic, and chemical properties. As Ge is deposited on Si(001), a surface layer consisting of a mixture of Ge and Si is speculated to form below 1 ML (monolayer) coverage; the atomistic process of Ge incorporation and the compositional distribution are unclear [8,14]. Above 1 ML coverage, the surface is expected to be terminated completely by Ge, based on surface energy consideration. Medium-energy ion scattering measurements [6] suggest different depth distributions of Ge on Si(001) at different growth temperatures. The actual distribution of Ge in the subsurface regions, however, is difficult to ascertain. This lack of knowledge of stoichiometry makes impossible a precise assignment of contributions to the morphology and stress modification as Ge is added. To our knowledge, no theoretical study has been done to address this important issue.

In this Letter, we present a comprehensive theoretical study of surface morphology and surface stress anisotropy of Ge-covered Si(001) as the amount of Ge is changed. We establish the most probable Ge subsurface stoichiometry above 1 ML coverage by matching the theory to the existing experimental information on surface morphology and surface stress anisotropy. We show that Ge deposited at typical rates and growth temperatures of 500–700 °C produces films that are not in the thermodynamic ground state, even if the deposited film is annealed at typical laboratory conditions. We conclude, as a consequence, that the reversal of surface stress anisotropy is caused by the behavior of the  $2 \times N$  reconstruction, with no substantial contribution from interlayer mixing.

Si(001) exhibits a  $2 \times 1$  reconstruction [15,16]. Surface atoms form dimer rows to lower the surface energy by eliminating one dangling bond per atom at the expense of introducing an additional anisotropic surface stress. The stress along the dimer bond is tensile, while the stress along the dimer row is compressive or at least less tensile [17]. This surface stress anisotropy leads to a stress-domain morphology with nearly equal population of  $2 \times 1$  and  $1 \times 2$  domains separated by monatomic steps [1,2]. By applying an external stress and measuring the change of relative concentration of the two domains, the intrinsic surface stress anisotropy on Si(001) has been quantitatively determined [18]. Scanning tunneling microscopy (STM) measurements on Ge-covered Si(001) show, similarly, that the intrinsic surface stress anisotropy is modified by Ge adsorption [13]. The anisotropy first decreases, becomes zero at about 1 ML coverage, and then increases in the opposite direction as the coverage increases. It is speculated that the development of the  $2 \times N$  reconstruction plays a major role in reversing the stress anisotropy, and that Ge/Si interlayer mixing and dimer buckling may contribute as well [13].

In order to explore these possibilities, we have calculated surface energies surface stress tensors of Si(001) as a function of Ge coverage. At a given coverage, the effect of interlayer mixing is investigated for several different Ge depth distributions. For each distributions, we determine the most stable surface structure (the value  $N$  in the  $2 \times N$  reconstruction) from a minimization of the

energy, and then calculate its corresponding surface stress anisotropy. We describe how the surface stress and the surface structure evolve as the Ge coverage increases. By comparing the calculated surface structures and their surface stress anisotropies to the experiment, we infer the most probable Ge stoichiometry profile in the near-surface region.

In calculating the properties of the  $2 \times N$  reconstructed surfaces, we opted to use the empirical Tersoff potential [19], as it is still prohibitive to carry out a series of first-principles calculations for a structure this complex. To test the validity of this empirical potential for our application, we first calculated surface energies and surface stress tensors for the  $2 \times 1$  structure of clean Si(001) and Si(001) covered by 1 and 2 ML of Ge, using both the first-principles pseudopotential total-energy method and the empirical potential, recognizing that the  $2 \times 1$  structure does not represent reality for this system. The details of the calculations will be published elsewhere [20].

To describe the surface stress tensor, we set the  $x$  direction along the dimer bond and the  $y$  direction along the dimer row. A positive stress tensor defines tensile stress. In Table I we compare the results from the two different potentials. The quantitative agreement between the two methods is rather good for surface energies, but less satisfactory for absolute values of surface stress tensors and anisotropies. Nevertheless and most importantly, the empirical potential predicts the quantitatively correct trend of change in all three stress quantities as a function of Ge coverage. Both calculations show the surface stress changes toward compression in both the  $x$  and  $y$  directions upon Ge deposition, reflecting the buildup of stress in the deposited film due to lattice mismatch. But the surface stress anisotropy remains essentially constant. At 2 ML coverage, we also considered the possibility of Ge/Si interlayer mixing, allowing the second layer of Ge to segregate to the energetically more favorable sites in the third and fourth layers (see discussion below). The surface energy is indeed reduced, but the surface stress anisotropy does not change noticeably. Therefore, *with or without*

*Ge/Si interlayer mixing, the surface stress anisotropy would not be reversed by Ge deposition if the surface maintained a  $2 \times 1$  reconstruction.*

Using now the empirical potential, we investigated how the surface stress anisotropy is affected by  $2 \times N$  reconstruction, caused by the ordering of dimer vacancies [3,5]. In creating the dimer vacancy, the more stable rebounded structure [4,21] was used. In Fig. 1 we plot the surface energy for the  $2 \times N$  reconstructed surface as a function of  $N$  for Ge coverages of 1, 1.5, and 2 ML. At 1 ML coverage, the Ge adatoms form the surface layer because the dangling-bond energy of Ge is much lower than that of Si [8,14]. For coverages above 1 ML, we consider two extreme cases: one at the thermodynamic limit, the other at the kinetic limit.

At typical growth and annealing temperatures of 500–700 °C, the effect of bulk diffusion is negligible [7]. The Ge adatoms, however, may still be able to segregate into the subsurface region through surface diffusion, which may be enhanced by the surface dimerization induced nonuniform stress field distribution in the subsurface region [22,23]. In Fig. 2 we draw a schematic side view diagram of the  $2 \times 1$  structure at 1 ML Ge coverage and mark the calculated atomic displacements (left half) and effective atomic stresses (right half). The surface dimer experiences a very small tensile stress. The second layer is under large compression. In the third and fourth layers, the sites beneath the surface dimers are under compressive stress and the sites between the surface dimers are under tensile stress. Below the fourth layer, there is virtually no stress. Because Si is smaller than Ge, lattice sites under compression favor Si occupancy and lattice sites under tension favor Ge. We therefore assume, as a reasonable thermodynamic limit, that for 1.5 ML coverage half a monolayer of Ge occupies the fourth-layer tensile sites with 1 ML on the surface; for 2 ML coverage a half monolayer each of Ge occupies both third- and fourth-layer tensile sites. At finite temperature entropy requires some Ge to occupy the unfavorable sites, but we find that the results are insensitive to this effect after testing several

TABLE I. Surface energies ( $\gamma$ ), stress tensors ( $\sigma$ ), and stress anisotropies ( $F$ ) of  $2 \times 1$  Ge-covered Si(001) calculated from the first-principles and the empirical (values in parentheses) potentials. A negative sign indicates compression. The last row takes into account possible Ge/Si interlayer mixing (see text for details).

Coverage	$\gamma$ (eV/Å <sup>2</sup> )	$\sigma_{xx}$ (eV/Å <sup>2</sup> )	$\sigma_{yy}$ (eV/Å <sup>2</sup> )	$F$ (eV/Å <sup>2</sup> )
0	0.0995 (0.0926)	0.073 (0.032)	-0.129 (-0.078)	0.202 (0.110)
1 ML	0.0963 (0.0848)	0.072 (0.019)	-0.155 (-0.092)	0.227 (0.110)
2 ML	0.1009 (0.0909)	0.024 (-0.008)	-0.166 (-0.143)	0.190 (0.135)
2 ML(s)	0.948 (0.0860)	0.018 (-0.029)	-0.185 (-0.143)	0.203 (0.114)

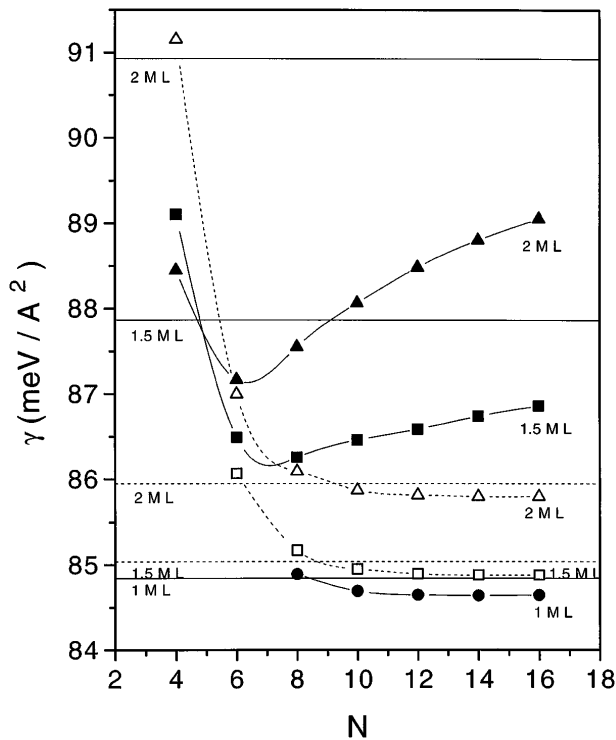


FIG. 1. Surface energies for the  $2 \times N$  reconstruction at various Ge coverages. Symbols are calculated values for 1 ML (solid circles), 1.5 ML (solid and open squares), and 2 ML (solid and open triangles) coverages, respectively. Solid (no interlayer mixing) and dashed curves (with interlayer mixing) are spline fits to the data. Horizontal lines mark the  $2 \times 1$  surface energies for each individual surface.

different occupational configurations. As a kinetic limit, we assume no Ge/Si interlayer mixing. All the deposited Ge adatoms are simply placed in the outer layers, for all coverages above 1 ML.

The optimal  $2 \times N$  reconstructions (the lowest-energy point) at the three coverages we considered are all more stable than the corresponding  $2 \times 1$  structures (horizontal lines in Fig. 1). The deposited films allowing interlayer mixing (the thermodynamic limit, dashed lines in Fig. 1) as expected have lower surface energy than the corresponding ones without interlayer mixing (solid lines). For the thermodynamic limit, the optimal value of  $N$  is independent of Ge coverage and remains in the vicinity of 14 with a very shallow well. Obviously Ge segregation lowers the surface energy by occupying the favorable atomic sites to release surface stress. The relaxation of the stress in turn reduces the concentration of dimer vacancies, leading to surface structures with unchanged (and large) values of  $N$  at different coverages. Experiments [3,9], however, indicate a changing  $N$  with Ge coverage, suggesting that the thermodynamic limit is an incorrect assumption. We therefore infer that the Ge/Si interlayer mixing is suppressed by a large kinetic barrier. The films grown at the experimental temperature (500–700 °C) [13] are apparently un-

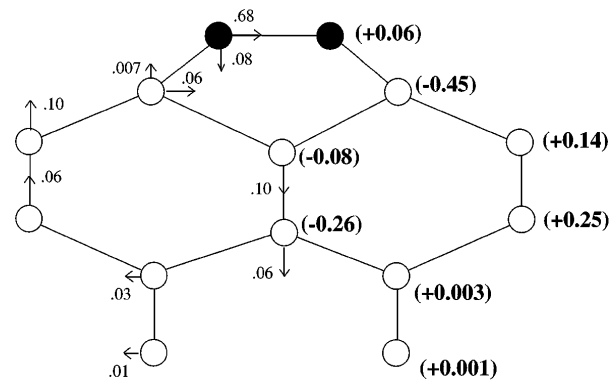


FIG. 2. Schematic side view of  $2 \times 1$  surface, projected to (110) plane. Solid circles are surface Ge atoms. Open circles are Si atoms. Arrows mark the direction of atomic displacements. Numbers on the left-hand side of the figure label the atomic displacements from their ideal bulk positions in Å. Numbers on the right-hand side of the figure are atomic-level stresses. The results are obtained using the empirical potential. The optimal structure agrees well with the present and a previous *ab initio* study [J. Cho and M. Kang, Phys. Rev. B **49**, 13 670 (1994)].

able to reach the thermodynamic ground state. Without interlayer mixing (solid lines in Fig. 1), the periodicity ( $N$ ) gradually decreases with increasing Ge coverage, indicating that more and more dimer vacancies are formed to release the increasing lattice-mismatch-induced compressive stress along dimer rows, consistent with both low energy electron diffraction (LEED) [3] and STM [9] observations. The calculated optimal  $N$  values are 14, 8, and 6 at coverages of 1, 1.5 and 2 ML, respectively, which agrees reasonably well with the experimental value of 12 at 0.9 ML, 10 at 1.6 ML, and 8 at 2.3 ML (LEED) [3] or 11 at 0.8 ML and 9 at 1.6 ML (STM) [9]. Moreover, the potential well around the optimal periodicity becomes deeper and narrower at the larger coverages, suggesting that the statistical distribution of  $N$  will become narrower with increasing coverage, as shown by STM [9]. The good agreement between experiment and the results at the kinetic limit suggest that surface morphology is dominated by kinetics, at least for Ge coverages above 1 ML.

The calculations of stress anisotropy confirm this conclusion. We calculated surface stress anisotropies for the surface structures having the optimal value of  $N$  as a function of Ge coverage. The results are compared to the experiment [13] in Fig. 3. In the thermodynamic limit, in addition to the formation of dimer vacancies, the stress field in the surface region is relaxed by interlayer mixing as the Ge coverage increases. As a result, the concentration of dimer vacancies does not increase with Ge coverage. The calculated surface stress anisotropy never changes sign, in disagreement with experiment. Without interlayer mixing, the theory shows that as the Ge coverage increases, the surface stress anisotropy decreases and reverses in sign at about 1.1 ML, in good agreement

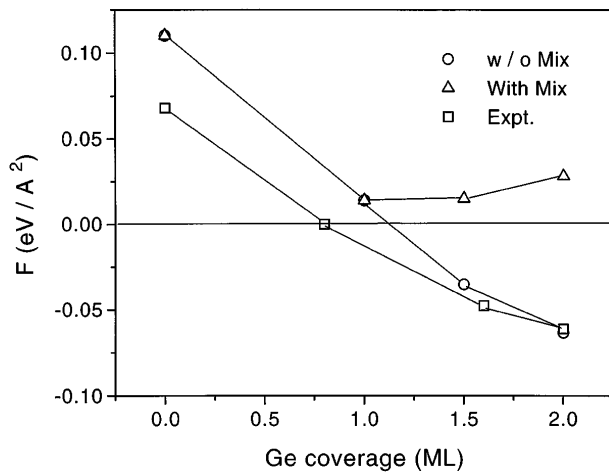


FIG. 3. Surface stress anisotropy as a function of Ge coverage. Open triangles and circles are calculated results for the optimized  $2 \times N$  reconstructed surface with and without interlayer mixing, respectively. Open squares are experimental data. Lines have been drawn to connect data points for clarity.

with experiment [13]. The reversal of the anisotropy is mainly caused by the formation of ordered dimer vacancies, which not only initially relieve the compressive stress along dimer rows but overcompensate at high dimer vacancy concentration so that the stress along dimer rows becomes tensile. The calculations also show that the rebonding of four second-layer atoms beneath the vacancy reinforces the effect by introducing a large tensile stress along the dimer row.

The analysis of both surface reconstruction and surface stress anisotropy therefore implies that Ge/Si(001) surfaces routinely produced by MBE deposition of Ge and observed by surface science techniques represent a state near the kinetic limit. The Ge/Si interlayer mixing cannot be substantial. To be certain, we performed two more calculations for the 2 ML coverage, assuming 12.5% and 25.0% of Ge segregates from the second layer to the third layer, respectively. With 12.5% Ge segregation, we find an optimal  $N$  value of 8 and a stress anisotropy of  $-0.22 \text{ eV}/\text{\AA}^2$ . The  $N$  value of 8 agrees better with the experimental value of 8 [3] or 9 [9] than the  $N$  value of 6 at the absolute kinetic limit; the stress anisotropy agrees less well with experiment but at least still has the correct negative sign. With 25.0% Ge segregation, we find an optimal  $N$  value of 10, which may still be acceptable, but the stress anisotropy becomes positive, in contradiction to the experiment. We expect the actual amount of Ge mixing to lower layers to be below 25.0% in the films grown experimentally [13].

In summary, we have calculated the surface energies and surface stress tensors of Ge-covered Si(001). We obtain the optimal structure and stress for the thermodynamic limit and for several kinetic limits. By comparing the theory to experiment, we conclude that the structures

and stress tensors routinely observed in experiment correspond to surfaces with minimal Ge/Si interlayer mixing; the resultant film is not in the thermodynamic ground state. For 2 ML coverage of Ge less than one-fourth of a layer can be mixed into the Si substrate. The small amount of intermixing suggests that barriers to interdiffusion are sufficiently high even with the added driving force of stress to prevent reaching the thermodynamic ground state at typical molecular beam epitaxy processing conditions.

We thank Fang Wu for helpful discussions. We are grateful for time on the Intel Paragon at Oak Ridge National Laboratory. This work was supported by NSF, Grants No. DMR93-04912 and No. DMR91-21074.

- [1] F.-K. Men, W.F. Packard, and M.B. Webb, *Phys. Rev. Lett.* **61**, 2469 (1988).
- [2] O.L. Alerhand, D. Vanderbilt, R.D. Meade, and J.D. Joannopoulos, *Phys. Rev. Lett.* **61**, 1973 (1988).
- [3] U. Köhler, O. Jusko, B. Müller, M. Horn-von Hoegen, and M. Pook, *Ultramicroscopy* **42-44**, 832 (1992).
- [4] J. Tersoff, *Phys. Rev. B* **45**, 8833 (1992).
- [5] X. Chen, F. Wu, Z.Y. Zhang, and M.G. Lagally, *Phys. Rev. Lett.* **73**, 850 (1994).
- [6] M. Copel, M.C. Reuter, M. Horn von Hoegen, and R.M. Tromp, *Phys. Rev. B* **42**, 11 682 (1990).
- [7] J. Tersoff, *Phys. Rev. B* **43**, 9377 (1991).
- [8] R.M. Tromp, *Phys. Rev. B* **47**, 7125 (1993).
- [9] F. Wu, X. Chen, Z.Y. Zhang, and M.G. Lagally, *Phys. Rev. Lett.* **74**, 574 (1995).
- [10] J. Tersoff, Y.H. Phang, Z.Y. Zhang, and M.G. Lagally, *Phys. Rev. Lett.* **75**, 2730 (1995).
- [11] Y.-W. Mo, D.E. Savage, B.S. Swartzentruber, and M.G. Lagally, *Phys. Rev. Lett.* **65**, 1020 (1990).
- [12] A. Sakai and T. Tostumi, *Phys. Rev. Lett.* **71**, 4007 (1993).
- [13] F. Wu and M.G. Lagally, *Phys. Rev. Lett.* **75**, 2534 (1995).
- [14] L. Patthey, E.L. Bullock, T. Abukawa, S. Kono, and L.S.O. Johansson, *Phys. Rev. Lett.* **75**, 2538 (1995).
- [15] R. Schlier and H. Farnsworth, *J. Chem. Phys.* **30**, 917 (1959).
- [16] R.M. Tromp, R.J. Hamers, and J.E. Demuth, *Phys. Rev. Lett.* **55**, 1303 (1985).
- [17] A. Garcia and J.E. Northrup, *Phys. Rev. B* **48**, 17 350 (1993).
- [18] M.B. Webb, F.-K. Men, B.S. Swartzentruber, R. Kariotis, and M.G. Lagally, *Surf. Sci.* **242**, 23 (1991).
- [19] J. Tersoff, *Phys. Rev. B* **39**, 5566 (1989).
- [20] Feng Liu (to be published).
- [21] K.C. Pandey, in *Proceedings of the Seventeenth International Conference on the Physics of Semiconductors*, edited by J.D. Chadi and W.A. Harrison (Springer-Verlag, New York, 1985), p. 55.
- [22] V. Vitek and T. Egami, *Phys. Status Solidi (b)* **144**, 145 (1987).
- [23] F.K. LeGoues, V.P. Kesan, S.S. Iyer, J. Tersoff, and R. Tromp, *Phys. Rev. Lett.* **64**, 2030 (1990).